Submicron Colloidosomes of Tunable Size and Wall Thickness

Grzegorz Sobczak,[†] *Tomasz Wojciechowski*[‡] *and Volodymyr Sashuk*[†]*

† Institute of Physical Chemistry, Polish Academy of Sciences, Kasprzaka 44/52, 01-224, Warsaw, Poland

‡ Institute of Physics, Polish Academy of Sciences, Al. Lotników 32/46, 02-668, Warsaw, Poland

ABSTRACT

We present a simple method for the fabrication of capsules of different sizes ranging from below 100 nm up to one micron. The capsules are produced by assembling gold nanoparticles at the interface of emulsion droplets. The size of the capsules is regulated by tuning the wetting properties of the nanoparticles through changing either the composition of their ligand shell or the composition of the oleic phase. The modified wettability affects not only the size, but also the thickness of capsule walls. The wall can be thin made of a single layer of the nanoparticles, or thick composed of multilayers. The durability of such capsules is quite high, though can be improved by chemical cross-linking with UV light. Also, the capsules are very tight, so that they can store a molecular cargo and then release it on demand.

INTRODUCTION

Hollow structures composed of nanoparticles (NPs), most known as colloidosomes or simply capsules, represent an attractive class of materials with potential applications in catalysis[1-14] and delivery systems.[15-21] The NP wall provides the mechanical stability of these structures and serves as a physical barrier between its interior and surrounding medium. Under external stimuli the wall of the capsule can stretch and shrink to encapsulate the chemical or biological species, and then disrupt to release them. The limited transport of substances across the wall enables also to selectively perform chemical reactions, especially when the NPs are imparted with catalytic functions.

The size of the capsule and the wall thickness are crucial for the above applications. Generally, the smaller the capsule and the thinner the wall, the better. In catalysis, a smaller size and thinner wall means higher active surface and faster substrate and product exchange. In turn, in drug delivery, a thin wall facilitates its disruption, while small dimensions enable the capsule to freely diffuse through endothelium and tissues and prevent it from being captured by macrophages.

The simplest way to build the capsules is to assemble the NPs on the interface of emulsion droplets.[22-28] The adsorption of NPs at the interface is described by the Pieranski equation:

$$\Delta E = \pi r^2 \gamma_{o/w} (1 - cos\theta_{o/w})^2$$

where, r is the radius of the NP, $\gamma_{o/w}$ the interfacial tension between oil and water, and $\theta_{o/w}$ the contact angle of the NP at the interface.

The process of the assembly is spontaneous and most favorable in terms of the reduction of the interfacial energy (ΔE) if the surface of NP is equally wetted by oil and aqueous phases, that is,

if the contact angle ($\theta_{o/w}$) of the NP at the interface approaches 90°. In this case the NPs are preferred to stay at the interface and the resulting droplets are the most stable against the coalescence.

Apart from the wettability the stability of emulsion droplets is also dependent on the pressure balance (ΔP) between the inside and the outside of droplet given by the Young-Laplace equation:

$$\Delta P = \frac{2\gamma_{o/w}}{R}$$

where R is the radius of the droplet.

When the size of droplets goes down an additional stabilization is required to assure the integrity of the resulting structures. Usually it is achieved by cross-linking the NPs *via* covalent or coordination chemistry.[3, 29-37] In the case of submicron droplets, the stabilization proves to be extremely challenging. To date, such droplets (capsules) were produced exclusively through electrostatic stabilization between charged NPs. This approach is applicable for both oppositely[38] and likely[15, 39-42] charged NPs. In the latter case, the repulsive interactions are mitigated by extraneous additives, e.g. surfactants.

Herein we present a practical route to fabricate ultrasmall capsules from electrically neutral NPs of amphiphilic nature. The strategy is based on the fine-tuning of the NP wettability. In this way we can control not only the size of the capsules, but also the thickness of their walls. The wetting properties of NPs are regulated orthogonally by altering either the polarity of oil phase or the composition of NP ligand shell. An appropriate polarity of oil phase is achieved by simply mixing two hydrocarbon solvents. The composition of NP ligand shell is established autonomously by *in situ* ligand exchange. Depending on the method used the capsules of

different size and the wall thickness are produced. The resulting capsules are superbly stable in aqueous solutions and their size is not changing over time. They are disintegrated only in chlorinated solvents. The wall of the capsule can be reinforced making it resistant to any solvent. Under UV irradiation the adjacent NPs are covalently cross-linked forming an impenetrable membrane. This allows to encapsulate small organic molecules inside the capsule and then release them upon chemical activation.

EXPERIMENTAL SECTION

Materials

$HAuCl_4 \cdot 3H_2O$ (gold (III) chloride trihydrate, ≥99.9%, Aldrich), DDA (dodecylamine, 98%, Aldrich), DDAB (didodecyldimethylammonium bromide, >98%, TCI), TBAB (tetrabutylammonium borohydride, 98%, Alfa Aesar), $NH_2NH_2 \cdot H_2O$ (hydrazine monohydrate, 98%, Alfa Aesar), MAA (methacrylic acid, 99%, Aldrich), BUD (11-bromo-1-undecanol, 97%, Alfa Aesar), DMAP (4-(dimethylamino)pyridine, ≥99.0%, Fluka), EDA (ethylenediamine, ≥99%, Aldrich), DCC (dicyclohexylcarbodiimide, 99%, Aldrich), MUTEG ((11-mercaptoundecyl)tetra(ethylene glycol), 90%, Aldrich), CaH_2 (calcium hydride, 92%, Alfa Aesar), KOH (potassium hydroxide, A.R., Chempur), KEX (potassium ethyl xanthogenate, 96%, Aldrich), TDS (trichlorododecylsilane, ≥95.0%, Aldrich), toluene (A.R., Chempur), acetone (A.R., Stanlab), chloroform (A.R., Chempur), DCM (methylene chloride, A.R., Stanlab), ethyl acetate (A.R., Stanlab), methanol (A.R., Chempur), THF (tetrahydrofuran, A.R., Poch), wide hexane fraction (Stanlab), and hexadecane (92%, Alfa Aesar) were used as received unless otherwise noted. Methylene chloride was dried over CaH_2 and distilled under argon atmosphere.

Methanol was dried over 3Å molecular sieves and distilled under argon atmosphere. Petroleum ether was distilled from wide hexane fraction. Hydrazine was dehydrated over KOH and distilled under argon atmosphere. Deionized water (18.3 MΩ·cm) was obtained from Milli-Q station. Gold (111) on mica was purchased from Phasis. Silicon wafers were purchased from ITME (Warsaw). Hydrophobic glass vials were prepared by soaking in TDS solution.[43]

Preparation and characterization of ligands and NPs

General. The experiments were performed at room temperature if not stated otherwise. The progress of organic reactions was monitored by thin layer chromatography (TLC) using Merck silica gel 60 F254 (0.2 mm) on alumina plates. The products were purified by column chromatography (CC) using Merck silica gel 60 (230-400 mesh ASTM) and then identified by NMR and MS techniques. NMR spectra were recorded on a Bruker (400 MHz) instrument. The chemical shifts (δ) are given in ppm relative to TMS, coupling constants are (J) in Hz. MS spectra were recorded on a Maldi SYNAPT G2-S HDMS (Waters) spectrometer.

Synthesis of 11-((ethoxycarbonothioyl)thio)undecyl methacrylate (XUMA)

The ligand was prepared in two steps through Steglich esterification followed by nucleophilic substitution: Briefly, a heat gun dried Schlenk flask charged with BUD (5.02 g, 20 mmol), MAA (1.7 mL, 20 mmol) and DMAP (0.49 g, 4 mmol) was evacuated in vacuo, flushed with argon and filled with 120 mL of dry DCM. The flask was placed into an ice water bath and a solution of DCC (4.54 g, 22 mmol) in dry DCM (40 mL) was added dropwise under magnetic stirring over 20 minutes. The reaction mixture was allowed to warm to room temperature and stirred for additional 24 h. The solvent was evaporated off, and the crude product was purified by CC

(petroleum ether : ethyl acetate = 98 : 2) to give 11-bromoundecyl methacrylate (BUMA) as a colorless oil with 62% yield.

^{1}H NMR (400 MHz, $CDCl_3$): δ 6.09 (s, 1H) 5.53 (s, 1H), 4.13 (t, J = 6.7 Hz, 2H), 3.51 (q, J = 7.4 Hz, 2H), 1.94 (s, 3H), 1.81−0.62 (m, 18H).

^{13}C NMR (100 MHz, $CDCl_3$): δ 167.5, 136.6, 125.0, 64.8, 33.9, 32.8, 29.4, 29.4, 29.4, 29.2, 28.7, 28.6, 28.1, 25.9, 18.3.

Next, a solution of BUMA (1.00 g, 3.13 mmol) in acetone (5 mL) was added dropwise to KEX (1.25 g, 77.83 mmol) dissolved in 35 mL of acetone and the mixture was stirred for 1 h. The potassium bromide was filtered off and the solution was concentrated on rotavap. The residue was chromatographed using petroleum ether as eluent to afford XUMA as an yellowish oil with 74% yield.

^{1}H NMR (400 MHz, $CDCl_3$): δ 6.09 (s, 1H) 5.53 (s, 1H), 4.65 (q, J = 7.1 Hz, 2H), 4.13 (t, J = 6.7 Hz, 2H), 3.11 (t, J = 7.5 Hz, 2H), 1.94 (s, 3H), 1.73−1.16 (m, 21H).

^{13}C NMR (100 MHz, $CDCl_3$): δ 215.3, 167.5, 136.6, 125.0, 69.7, 64.8, 35.9, 29.4, 29.4, 29.4, 29.2, 29.1, 28.9, 28.6, 28.3, 26.0, 18.3, 13.8.

HRMS (ESI): m/z: calcd for $C_{18}H_{32}O_3S_2Na$: 383.1691 $[M+Na]^+$; found: 383.1684.

Synthesis of 11-mercaptoundecyl methacrylate (MUMA)

MUMA was synthesized by cleaving the XUMA xanthate group: Briefly, a heat gun dried Schlenk flask charged with XUMA (0.50 g, 1.39 mmol) was evacuated and backfilled with argon. The substrate was dissolved in dry methanol and EDA (174 μL) was injected. The

reaction mixture was stirred for half an hour and then concentrated on rotavap. To prevent oxidation the residue was immediately subjected to CC (petroleum ether : ethyl acetate = 99 : 1) to give MUMA as a colorless oil with 38% yield.

^{1}H NMR (400 MHz, $CDCl_3$): δ 6.08 (s, 1H) 5.53 (s, 1H), 4.13 (t, J = 6.7 Hz, 2H), 2.51 (q, J = 7.5 Hz, 2H), 1.94 (s, 3H), 1.79−1.19 (m, 18H). The NMR data are in agreement with those published in literature.[44]

Synthesis and functionalization of gold NPs (AuNPs)

AuNPs with a core size of about 5 nm were synthesized using a seeding growth method described by Jana et al.[45] First, DDAB stock solution was prepared by dissolving DDAB (1.39 g) in 30 mL of toluene under sonication. Note: the ultrasound was used also for the dissolution of substrates in the subsequent stages of the synthesis. Preparation of seeding solution: $HAuCl_4 \cdot 3H_2O$ (20 mg) was dissolved in the presence of DDA (180 mg) in 5 mL of the DDAB solution and then reduced by TBAB (50 mg dissolved in 2 mL of the DDAB solution) added at once under vigorous stirring. The stirring was continued for additional 1 h. The formation of gold seeds was manifested by the appearance of brown red color. Preparation of growth solution: $HAuCl_4 \cdot 3H_2O$ (160 mg), DDA (1800 mg) and DDAB (1000 mg) were dissolved in 50 mL of toluene and combined with the seeding solution. To the vigorously stirred growth solution hydrazine (128 µL dissolved in 20 mL of the DDAB solution) was injected dropwise using a syringe without a plunger with a needle of ø=0.6 mm. After the reductant was added the mixture was left stirring overnight. The mixture turned dark red indicating the successful growth of gold NPs. The NPs were coated with thiolate ligands either using XUMA[46] or in the reaction with MUMA. In the latter case, the as-obtained gold NPs (13 g, 0.1 mmol in terms of gold) were

precipitated with methanol (40 mL) and the supernatant was carefully decanted using a glass pipette. The NP precipitate was redispersed in 2 mL of chloroform, and MUMA (0.1 mmol) was injected to the stirred NP dispersion. The reaction mixture was left stirring overnight. The NPs were precipitated with methanol (30 mL) and collected by centrifugation (5000 rpm, 5 min). The NP precipitate was redispersed in chloroform (1 mL), precipitated with methanol (30 mL) and centrifuged. The cycle of the dissolution, precipitation and centrifugation was repeated 7 times. Finally, the purified, MUMA-coated gold NPs were dried and dispersed in 5 mL of chloroform to give 20 mM NP dispersion.

Preparation and characterization of emulsions (capsules)

The NP dispersion (5 μL) was transferred into the hydrophobic vial and the solvent was removed in vacuo. The NP precipitate was redispersed in 3 μL of toluene with an admixture of auxiliary solvent (hexadecane) or ligand (MUTEG). Next, 1 mL of water was added and the biphasic mixture was sonicated using a Vibra-Cell processor (Sonics) with five 3-s pulses at 50% output making 15-s pause between each pulse. To cross-link the NPs the emulsion was diluted with 3 mL of water, transferred to quartz cuvette and irradiated twice for 6 min with a mercury-vapor lamp with average irradiance of 32 W/m^2 in UVC region.

Dynamic light scattering (DLS)

1 mL of the emulsion was transferred into a plastic cuvette. The hydrodynamic size of emulsion droplets (capsules) and their size distribution were measured on a Malvern Zetasizer NanoZS instrument.

Scanning electron microscopy (SEM)

A drop of the emulsion was put on the silicon plate and allowed to dry. SEM images were recorded on a FEI Nova NanoSEM 450 with an acceleration voltage of 5 kV. The capsules were cut with focused ion beam (FIB) and imaged using Zeiss Neon 40 Auriga CrossBeam system.

UV-Vis

1.5 mL of the emulsion was transferred into a quartz cuvette. UV-vis spectra were recorded on an Evolution 201 spectrophotometer from Thermo Scientific.

Encapsulation and release of molecular cargo

A solution of a perylene bisimide dye in toluene (2.7 mM, 0.33 μL) was combined with 5 μL of the NP dispersion. The solvent was evaporated and the residue was redispersed in 3 μL of 10% v/v solution of hexadecane in toluene. Next, 1 mL of water was added and the mixture was emulsified and then irradiated with UV light (see above). The capsules were purified by passing the emulsion through a Nylon syringe filter (pore size 0.22 μm) followed by extensive washing with water and 1,4-dioxane. To release the cargo, the capsules absorbed on the filter were rinsed with an aqueous solution of KCN (1 mg dissolved in 2 mL of water) and then with 2 mL of 1,4-dioxane.

Quantitative assessment of NP wettability

The wettability, given by the contact angle $\theta_{o/w}$, was estimated using macroscopic gold surface covered with self-assembling monolayers (SAMs) of thiolate ligands. Preparation of MUMA SAMs: the gold on mica was immersed into 2 mM ethanolic solution of MUMA for 48 h, rinsed

with ethanol and dried under argon. Preparation of mixed MUMA-MUTEG SAMs: the MUMA-coated gold was immersed into 20 pM ethanolic solution of MUTEG for 15 and 60 min, respectively, rinsed with ethanol and dried under argon. The SAMs-decorated gold was immersed into water and a droplet of oil was deposited by syringe. The shape of the droplet was recorded with a digital camera from Canon. The value of the contact angle was determined using ImageJ and DropSnake software. The results were averaged for at least three droplets deposited at different places on the surface.

RESULTS AND DISCUSSION

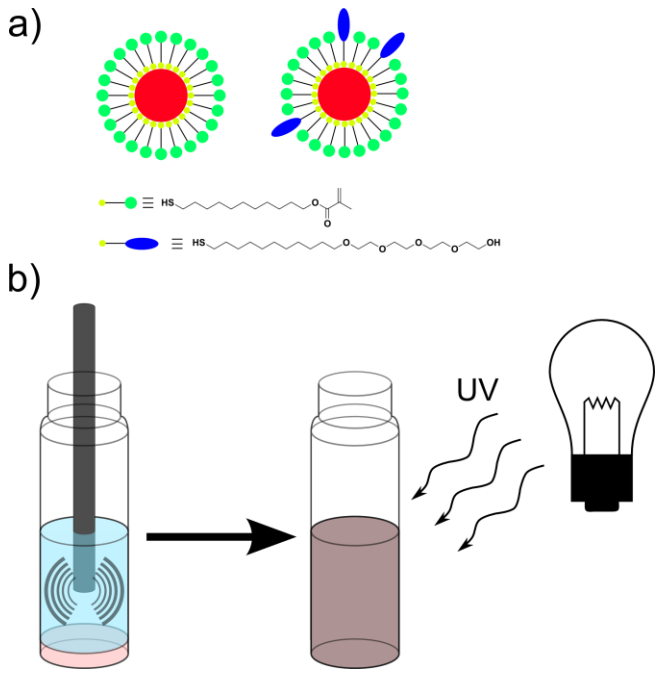

Figure 1. Cartoon representation of gold NPs used in our study (a) and experimental set-up for capsule preparation (b). The NPs were coated with a monolayer of thiolate ligands terminated with methacrylic groups (MUMA). These ligands were used alone or in combination with ligands ended by a polyethylene glycol moiety (MUTEG). The capsules were obtained by sonication of oleic NP dispersions in water followed by irradiation with UV light.

In our study we employed gold nanoparticles (AuNPs) covered with ester groups as a model system (Figure 1). Such NPs were shown previously to exhibit the propensity to segregate at liquid interfaces.[44, 47-50] We wondered how the modified wetting properties of the amphiphilic NPs would influence their interfacial behavior. The wettability was first tuned by changing the composition of dispersed phase. Water was used as a continuous phase. The attempts to prepare stable emulsion from chloroform in which the NPs were initially dispersed were failed. However, when chloroform was substituted with toluene, which is less polar solvent, the stable emulsion was readily formed. The emulsion was prepared by sonication. According to DLS the average droplet size was about 150 nm and did not change for several months (see Figure S1, Supporting Information). The emulsion was broken only after the addition of chloroform. In turn, in hexadecane, which is even less polar solvent than chloroform and toluene, the NPs aggregated. However, when toluene was admixed with hexadecane the emulsion was formed again. Remarkably, with increasing the content of hexadecane in toluene the droplet size increased. For example, for 5% v/v of hexadecane, the average size was about 500 nm. The dependency of the droplet size on the hexadecane content is shown in Figure 2a. To reveal the structure of the emulsion droplets, i.e. capsules, the scanning electron microscopy (SEM) was used. Unfortunately, during the sample preparation, the capsule rupture has occurred (Figure S2, Supporting Information). Therefore, before imaging, the capsules were reinforced by UV light. Upon irradiation the NPs were covalently cross-linked through polymerization of olefinic bonds pre-installed on their surface. After cross-linking the emulsion became resistant against chloroform indicating the high reaction efficiency. According to SEM the capsule structure was dependent on the solvent used. When the pure toluene was employed the NPs occupied not only the surface of the droplets, but also their interior forming a thick wall. With increasing the

hexadecane content the thickness of the wall decreased. At contents above 5% (v/v), the capsule wall was composed of as little as a single NP monolayer. The dependency of the wall thickness on the hexadecane content is presented in Figure 2b. The thickness of capsule walls was estimated from FIB snapshots. The rationale behind the observed dependencies is the change of wetting properties of the NPs. The wettability affects both the interfacial and the dispersing properties of the NPs. With increasing the content of hexadecane, the NPs more readily adsorb at the liquid interface. This follows from the contact angle measurements (Figure 2a) and experimental observations on the stability and interfacial coverage of droplets (capsules) at different NP concentrations (Figure S3). The influence of hexadecane on the interfacial adsorption is particularly seen at low NP loadings. The capsules obtained in the presence of hexadecane are usually more tightly packed with NPs than those prepared from toluene-water mixture (Figure S3). While the interfacial coverage is responsible for the tightness of the capsules, it does not noticeably affect their size. The capsule size depends rather on the wall thickness (Figure 2b). Apparently, the thicker the wall, the smaller the capsule, that indicates a steric factor in the emulsion stabilization. The wall thickness, in turn, is determined by the amount of the NPs dispersed in the oil phase. With increasing the content of hexadecane, the NP dispersibility, and hence, the wall thickness decreases. As already noted, at a certain hexadecane content, typically about 5%, the NPs remain only at the interface forming the monolayer while excess NPs precipitate out of the emulsion. Further dilution of toluene by hexadecane causes only an increase in the capsule size. For instance, at hexadecane content of 50%, the average size of capsules reaches 1 μm. The increase of the capsule size is the result of further drop of NP dispersibility. The fewer NPs are available in the emulsion, the smaller the interfacial area that can be covered by them, and therefore, the larger capsules are formed.

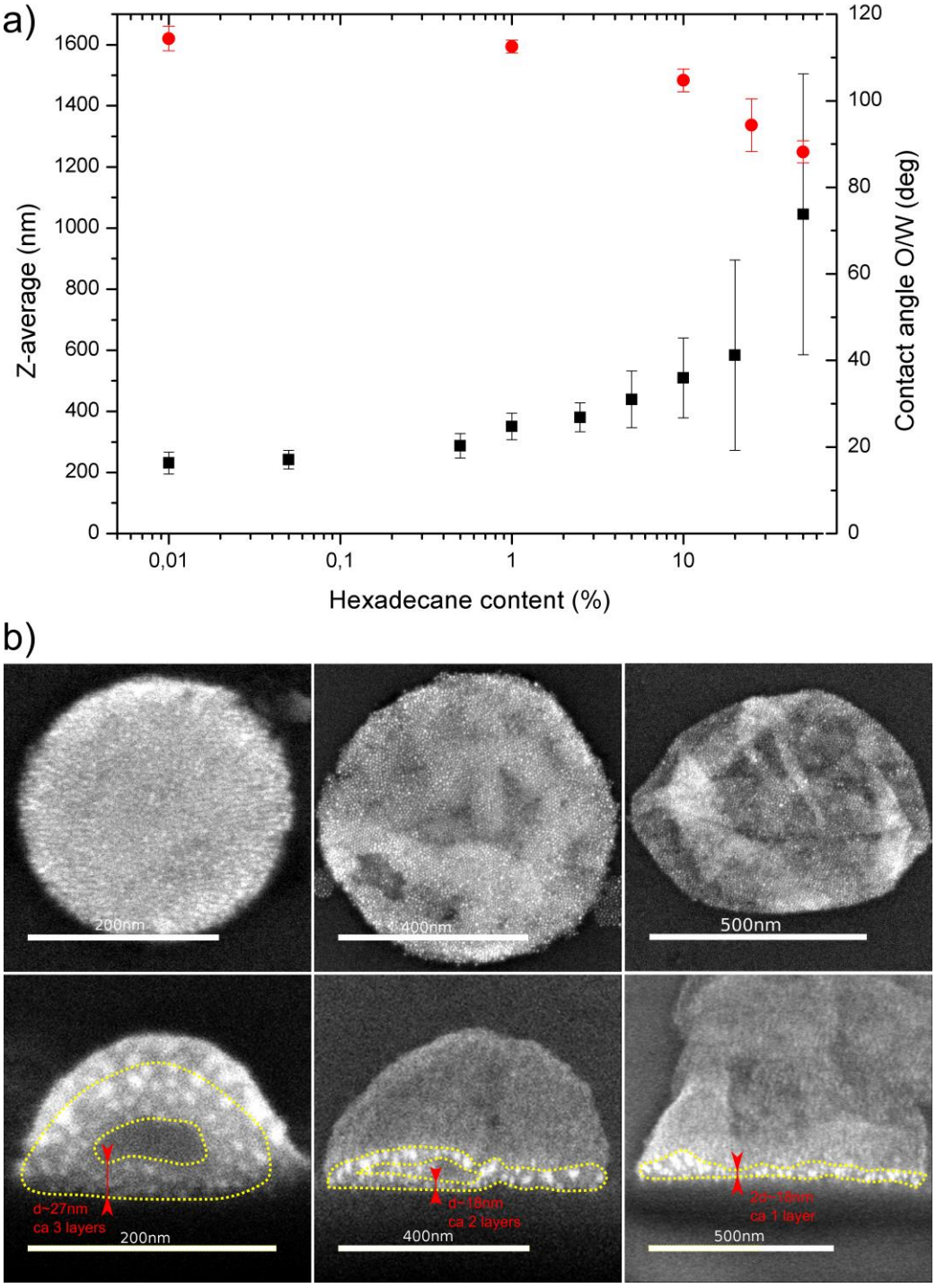

Figure 2. a) Plots of the dependencies of capsule size (*black dots*) and contact angle (*red dots*) on the content (v/v) of hexadecane in toluene phase; b) SEM images of capsules and their cross-sections for 0% (*left*), 1% (*middle*) and 5% (*right*) hexadecane content.

The wetting properties of the NPs can be also regulated by changing the composition of their ligand shell. To this end, an admixture of more polar ligand (MUTEG) was employed with toluene as a dispersed phase (Figure 1). The shell modification was accomplished *in situ* by ligand exchange. The amount of MUTEG used was up to 5 mol% in terms of ester ligands adsorbed on the NP surface. At higher MUTEG loadings, the NPs became too polar and migrated into the aqueous phase. As expected, the largest drop of contact angle was observed for 5 mol% MUTEG loading. The changes of contact angle induced by ligand-exchange are shown in Figure 3b. The ligand-exchange reaction, as followed from the kinetic traces, reached equilibrium within 15 minutes. As in the case of solvent mixing, the decrease of the contact angle impaired the dispersibility of the NPs in the oleic phase. In consequence, the capsules with thin walls of average thickness of the single NP monolayer were produced (Figure 3c). Remarkably, despite thin wall the capsules were much smaller than those obtained in the presence of hexadecane (Figure 3c). This result is easily rationalized in terms of interfacial activity. The NPs with heterogeneous coating stabilize the liquid interface much stronger than homogenous ones.[51-59]

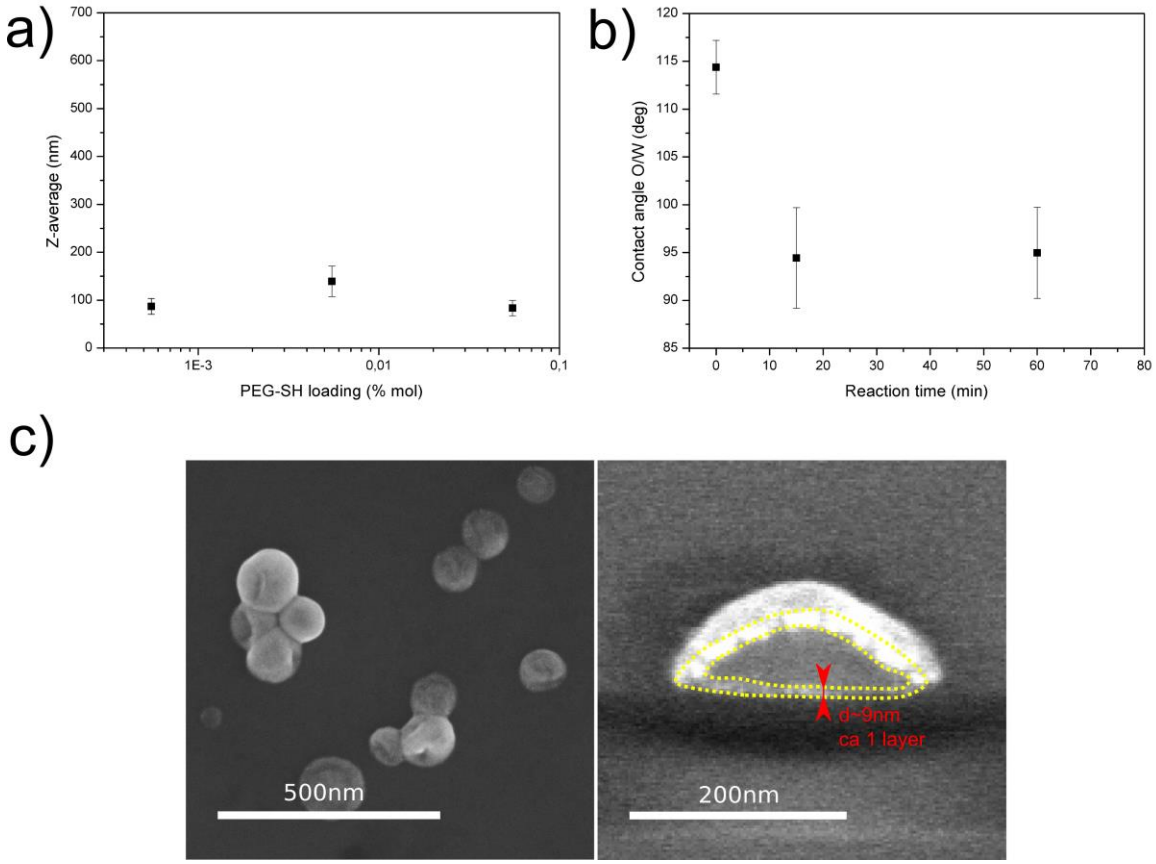

Figure 3. a) Plot of the dependency of capsule size on the amount of MUTEG used in the ligand exchange reaction; b) Time evolution of contact angle during the ligand exchange; c) SEM images of capsule(s) and its cross-section after the ligand exchange.

Interestingly, the effectiveness of the NPs in stabilizing the interface can also be gauged from UV-Vis spectra (Figure S4). Importantly, this can be done before the capsule reinforcement. The NPs exhibit a plasmon band whose shape and position depends on the average distance between the NPs.[60] In toluene, wherein the NPs are readily dispersed, the plasmon band after emulsification is barely changed. However, when the NPs are accommodated at the interface, the interparticle spacing is decreased and the electronic coupling becomes stronger causing the plasmon band to shift toward the red end of the spectrum.

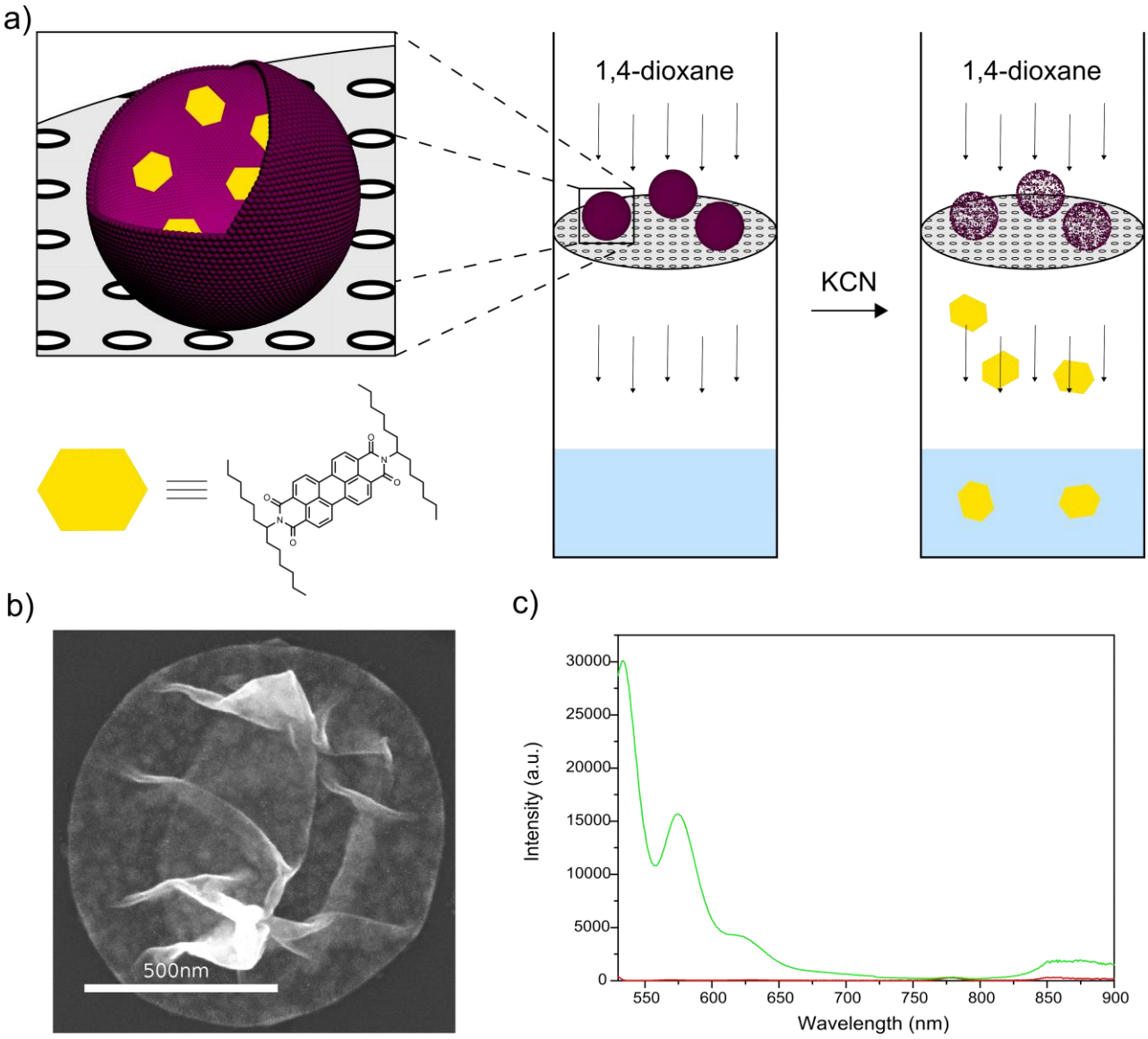

Figure 4. a) Illustration of cargo release after breaking the capsule walls with a chemical activator; b) SEM image of capsule loaded with the cargo. The image reveals that the capsule wall consists of the monolayer of hexagonally arranged NPs. The wrinkled structure indicates the presence of hollow interior; c) Fluorescence spectra of the permeate before (*red*) and after (*green*) breaking the capsule wall.

To examine the tightness, the capsules with the thinnest wall, that is, made of the single NP monolayer, were loaded with fluorescent dye (Figure 4a). The size of the cargo (width ~ 1.5 nm)

was comparable with the size of pores (diameter ~ 1.4 nm) left in the capsule wall after hexagonal close packing of the NPs. The pore diameter was calculated from the NP radius ($R=R_C+R_L$) as $d=0.31R$, where R_C is the radius of the metal core (2.5 nm), and R_L is the thickness of the ligand shell (1.99 nm). The capsules were deposited on the Nylon filter and washed with 1,4-dioxane. The presence of the dye in the permeate was monitored by fluorescence emission. After several washes no cargo leaching was detected. The cargo was released only after breaking (dissolving) the capsule walls with potassium cyanide (Figure 4c).

SUMMARY

We developed a straightforward method for the preparation of submicron capsules with tailorable size and wall thickness. The capsules are prepared from the emulsion droplets stabilized by NPs. The capsule size and the wall thickness are controlled by tuning the wetting properties of the NPs. If the NPs are better wetted by dispersed phase than continuous phase, the capsules of thick walls and small sizes are formed. In contrast, the NPs equally wetted by both phases produce the capsules with thin walls and variable sizes. In the latter case, the capsule size is dependent on the composition of their ligand shell. The NPs coated with two types of ligands stabilize much smaller capsules than those coated with one type of ligands. The obtained capsules, due to covalent cross-linking and hexagonal NP packing, are extremely robust and tight, even those composed of the single NP monolayer. This feature makes the capsules suitable for storage and easy release of tiny cargoes.

ASSOCIATED CONTENT

Supporting Information. SEM and DLS measurements of stability of capsules before and after cross-linking at various NP loadings, UV-Vis spectra of the NPs before and after emulsification with different additives. This material is available free of charge via the Internet at http://pubs.acs.org.

AUTHOR INFORMATION

Corresponding Author

E-mail: vsashuk@ichf.edu.pl

Author Contributions

The manuscript was written through contributions of all authors. All authors have given approval to the final version of the manuscript.

ACKNOWLEDGMENT

This work was financed by National Science Center (Grant Sonata UMO-2011/01/D/ST5/03518). The authors thank S. Iskorościńska for providing fluorescent dye.

REFERENCES

(1) Cao, W.; Huang, R.; Qi, W.; Su, R.; He, Z., Self-Assembly of Amphiphilic Janus Particles into Monolayer Capsules for Enhanced Enzyme Catalysis in Organic Media. *ACS Appl. Mater. Interfaces* **2015,** 7, 465-473.

(2) Samanta, B.; Yang, X.-C.; Ofir, Y.; Park, M.-H.; Patra, D.; Agasti, S. S.; Miranda, O. R.; Mo, Z.-H.; Rotello, V. M., Catalytic Microcapsules Assembled from Enzyme–Nanoparticle Conjugates at Oil–Water Interfaces. *Angew. Chem. Int. Ed.* **2009,** 48, 5341-5344.

(3) Jeong, Y.; Duncan, B.; Park, M.-H.; Kim, C.; Rotello, V. M., Reusable biocatalytic crosslinked microparticles self-assembled from enzyme-nanoparticle complexes. *Chem. Commun.* **2011,** 47, 12077-12079.

(4) Crossley, S.; Faria, J.; Shen, M.; Resasco, D. E., Solid Nanoparticles that Catalyze Biofuel Upgrade Reactions at the Water/Oil Interface. *Science* **2010,** 327, 68-72.
(5) Sun, S.; Li, M.; Dong, F.; Wang, S.; Tian, L.; Mann, S., Chemical Signaling and Functional Activation in Colloidosome-Based Protocells. *Small* **2016,** 12, 1920-1927.
(6) Chen, Z.; Zhao, C.; Ju, E.; Ji, H.; Ren, J.; Binks, B. P.; Qu, X., Design of Surface-Active Artificial Enzyme Particles to Stabilize Pickering Emulsions for High-Performance Biphasic Biocatalysis. *Adv. Mater.* **2016,** 28, 1682-1688.
(7) Chen, S.; Zhang, F.; Yang, M.; Li, X.; Liang, H.; Qiao, Y.; Liu, D.; Fan, W., A simple strategy towards the preparation of a highly active bifunctionalized catalyst for the deacetalization reaction. *Appl. Catal., A.* **2016,** 513, 47-52.
(8) Huang, J.; Cheng, F.; Binks, B. P.; Yang, H., pH-Responsive Gas–Water–Solid Interface for Multiphase Catalysis. *J. Am. Chem. Soc.* **2015,** 137, 15015-15025.
(9) Burdyny, T.; Riordon, J.; Dinh, C.-T.; Sargent, E. H.; Sinton, D., Self-assembled nanoparticle-stabilized photocatalytic reactors. *Nanoscale* **2016,** 8, 2107-2115.
(10) Ma, S.; Wang, Y.; Jiang, K.; Han, X., Decoratable hybrid-film-patch stabilized Pickering emulsions and their catalytic applications. *Nano Res.* **2015,** 8, 2603-2610.
(11) Pera-Titus, M.; Leclercq, L.; Clacens, J.-M.; De Campo, F.; Nardello-Rataj, V., Pickering Interfacial Catalysis for Biphasic Systems: From Emulsion Design to Green Reactions. *Angew. Chem. Int. Ed.* **2015,** 54, 2006-2021.
(12) Huang, J.; Yang, H., A pH-switched Pickering emulsion catalytic system: high reaction efficiency and facile catalyst recycling. *Chem. Commun.* **2015,** 51, 7333-7336.
(13) Chen, Z.; Zhou, L.; Bing, W.; Zhang, Z.; Li, Z.; Ren, J.; Qu, X., Light Controlled Reversible Inversion of Nanophosphor-Stabilized Pickering Emulsions for Biphasic Enantioselective Biocatalysis. *J. Am. Chem. Soc.* **2014,** 136, 7498-7504.
(14) Zhou, W.-J.; Fang, L.; Fan, Z.; Albela, B.; Bonneviot, L.; De Campo, F.; Pera-Titus, M.; Clacens, J.-M., Tunable Catalysts for Solvent-Free Biphasic Systems: Pickering Interfacial Catalysts over Amphiphilic Silica Nanoparticles. *J. Am. Chem. Soc.* **2014,** 136, 4869-4872.
(15) Yang, X.-C.; Samanta, B.; Agasti, S. S.; Jeong, Y.; Zhu, Z.-J.; Rana, S.; Miranda, O. R.; Rotello, V. M., Drug Delivery Using Nanoparticle-Stabilized Nanocapsules. *Angew. Chem. Int. Ed.* **2011,** 50, 477-481.
(16) Jiang, Y.; Tang, R.; Duncan, B.; Jiang, Z.; Yan, B.; Mout, R.; Rotello, V. M., Direct Cytosolic Delivery of siRNA Using Nanoparticle-Stabilized Nanocapsules. *Angew. Chem. Int. Ed.* **2015,** 54, 506-510.
(17) Shi, J.; Jiang, Y.; Wang, X.; Wu, H.; Yang, D.; Pan, F.; Su, Y.; Jiang, Z., Design and synthesis of organic-inorganic hybrid capsules for biotechnological applications. *Chem. Soc. Rev.* **2014,** 43, 5192-5210.
(18) Lu, C.-H.; Willner, I., Stimuli-Responsive DNA-Functionalized Nano-/Microcontainers for Switchable and Controlled Release. *Angew. Chem. Int. Ed.* **2015,** 54, 12212-12235.
(19) Kim, C. S.; Mout, R.; Zhao, Y.; Yeh, Y.-C.; Tang, R.; Jeong, Y.; Duncan, B.; Hardy, J. A.; Rotello, V. M., Co-Delivery of Protein and Small Molecule Therapeutics Using Nanoparticle-Stabilized Nanocapsules. *Bioconjugate Chem.* **2015,** 26, 950-954.
(20) Tang, R.; Kim, C. S.; Solfiell, D. J.; Rana, S.; Mout, R.; Velázquez-Delgado, E. M.; Chompoosor, A.; Jeong, Y.; Yan, B.; Zhu, Z.-J.; Kim, C.; Hardy, J. A.; Rotello, V. M., Direct Delivery of Functional Proteins and Enzymes to the Cytosol Using Nanoparticle-Stabilized Nanocapsules. *ACS Nano* **2013,** 7, 6667-6673.

(21) Zhou, S.; Fan, J.; Datta, S. S.; Guo, M.; Guo, X.; Weitz, D. A., Thermally Switched Release from Nanoparticle Colloidosomes. *Adv. Funct. Mater.* **2013,** 23, 5925-5929.
(22) Böker, A.; He, J.; Emrick, T.; Russell, T. P., Self-assembly of nanoparticles at interfaces. *Soft Matter* **2007,** 3, 1231-1248.
(23) Wang, D.; Duan, H.; Mohwald, H., The water/oil interface: the emerging horizon for self-assembly of nanoparticles. *Soft Matter* **2005,** 1, 412-416.
(24) Patra, D.; Sanyal, A.; Rotello, V. M., Colloidal Microcapsules: Self-Assembly of Nanoparticles at the Liquid–Liquid Interface. *Chem. Asian J.* **2010,** 5, 2442-2453.
(25) Hu, L.; Chen, M.; Fang, X.; Wu, L., Oil-water interfacial self-assembly: a novel strategy for nanofilm and nanodevice fabrication. *Chem. Soc. Rev.* **2012,** 41, 1350-1362.
(26) Popp, N.; Kutuzov, S.; Böker, A., Various Aspects of the Interfacial Self-Assembly of Nanoparticles. In *Complex Macromolecular Systems II*, Müller, E. A. H.; Schmidt, H.-W., Eds. Springer Berlin Heidelberg: Berlin, Heidelberg, 2010; pp 39-58.
(27) Niu, Z.; He, J.; Russell, T. P.; Wang, Q., Synthesis of Nano/Microstructures at Fluid Interfaces. *Angew. Chem. Int. Ed.* **2010,** 49, 10052-10066.
(28) Binder, W. H., Supramolecular Assembly of Nanoparticles at Liquid–Liquid Interfaces. *Angew. Chem. Int. Ed.* **2005,** 44, 5172-5175.
(29) Jeong, Y.; Chen, Y.-C.; Turksoy, M. K.; Rana, S.; Tonga, G. Y.; Creran, B.; Sanyal, A.; Crosby, A. J.; Rotello, V. M., Tunable Elastic Modulus of Nanoparticle Monolayer Films by Host–Guest Chemistry. *Adv. Mater.* **2014,** 26, 5056-5061.
(30) Hussain, I.; Zhang, H.; Brust, M.; Barauskas, J.; Cooper, A. I., Emulsions-directed assembly of gold nanoparticles to molecularly-linked and size-controlled spherical aggregates. *J. Colloid Interface Sci.* **2010,** 350, 368-372.
(31) Arumugam, P.; Patra, D.; Samanta, B.; Agasti, S. S.; Subramani, C.; Rotello, V. M., Self-Assembly and Cross-linking of FePt Nanoparticles at Planar and Colloidal Liquid−Liquid Interfaces. *J. Am. Chem. Soc.* **2008,** 130, 10046-10047.
(32) Samanta, B.; Patra, D.; Subramani, C.; Ofir, Y.; Yesilbag, G.; Sanyal, A.; Rotello, V. M., Stable Magnetic Colloidosomes via Click-Mediated Crosslinking of Nanoparticles at Water–Oil Interfaces. *Small* **2009,** 5, 685-688.
(33) Patra, D.; Pagliuca, C.; Subramani, C.; Samanta, B.; Agasti, S. S.; Zainalabdeen, N.; Caldwell, S. T.; Cooke, G.; Rotello, V. M., Molecular recognition at the liquid-liquid interface of colloidal microcapsules. *Chem. Commun.* **2009**, 28, 4248-4250.
(34) Duncan, B.; Li, X.; Landis, R. F.; Kim, S. T.; Gupta, A.; Wang, L.-S.; Ramanathan, R.; Tang, R.; Boerth, J. A.; Rotello, V. M., Nanoparticle-Stabilized Capsules for the Treatment of Bacterial Biofilms. *ACS Nano* **2015,** 9, 7775-7782.
(35) Skaff, H.; Lin, Y.; Tangirala, R.; Breitenkamp, K.; Böker, A.; Russell, T. P.; Emrick, T., Crosslinked Capsules of Quantum Dots by Interfacial Assembly and Ligand Crosslinking. *Adv. Mater.* **2005,** 17, 2082-2086.
(36) Lin, Y.; Skaff, H.; Böker, A.; Dinsmore, A. D.; Emrick, T.; Russell, T. P., Ultrathin Cross-Linked Nanoparticle Membranes. *J. Am. Chem. Soc.* **2003,** 125, 12690-12691.
(37) Tangirala, R.; Hu, Y.; Joralemon, M.; Zhang, Q.; He, J.; Russell, T. P.; Emrick, T., Connecting quantum dots and bionanoparticles in hybrid nanoscale ultra-thin films. *Soft Matter* **2009,** 5, 1048-1054.
(38) Li, S.; Moosa, B. A.; Croissant, J. G.; Khashab, N. M., Electrostatic Assembly/Disassembly of Nanoscaled Colloidosomes for Light-Triggered Cargo Release. *Angew. Chem. Int. Ed.* **2015,** 54, 6804-6808.

(39) Yeh, Y.-C.; Tang, R.; Mout, R.; Jeong, Y.; Rotello, V. M., Fabrication of Multiresponsive Bioactive Nanocapsules through Orthogonal Self-Assembly. *Angew. Chem. Int. Ed.* **2014,** 53, 5137-5141.
(40) Bollhorst, T.; Grieb, T.; Rosenauer, A.; Fuller, G.; Maas, M.; Rezwan, K., Synthesis Route for the Self-Assembly of Submicrometer-Sized Colloidosomes with Tailorable Nanopores. *Chem. Mater.* **2013,** 25, 3464-3471.
(41) Bollhorst, T.; Shahabi, S.; Wörz, K.; Petters, C.; Dringen, R.; Maas, M.; Rezwan, K., Bifunctional Submicron Colloidosomes Coassembled from Fluorescent and Superparamagnetic Nanoparticles. *Angew. Chem. Int. Ed.* **2015,** 54, 118-123.
(42) Sihler, S.; Schrade, A.; Cao, Z.; Ziener, U., Inverse Pickering Emulsions with Droplet Sizes below 500 nm. *Langmuir* **2015,** 31, 10392-10401.
(43) Sashuk, V.; Hołyst, R.; Wojciechowski, T.; Górecka, E.; Fiałkowski, M., Autonomous Self-Assembly of Ionic Nanoparticles into Hexagonally Close-Packed Lattices at a Planar Oil–Water Interface. *Chem. Eur. J.* **2012,** 18, 2235-2238.
(44) Zhang, X.; Liu, L.; Tian, J.; Zhang, J.; Zhao, H., Copolymers of styrene and gold nanoparticles. *Chem. Commun.* **2008**, 48, 6549-6551.
(45) Jana, N. R.; Peng, X., Single-Phase and Gram-Scale Routes toward Nearly Monodisperse Au and Other Noble Metal Nanocrystals. *J. Am. Chem. Soc.* **2003,** 125, 14280-14281.
(46) Sashuk, V., Thiolate-Protected Nanoparticles via Organic Xanthates: Mechanism and Implications. *ACS Nano* **2012,** 6, 10855-10861.
(47) Tian, J.; Zheng, F.; Duan, Q.; Zhao, H., Self-assembly of polystyrene with pendant hydrophilic gold nanoparticles: the influence of the hydrophilicity of the hybrid polymers. *J. Mater. Chem.* **2011,** 21, 16928-16934.
(48) Tian, J.; Liu, G.; Guan, C.; Zhao, H., Amphiphilic gold nanoparticles formed at a liquid-liquid interface and fabrication of hybrid nanocapsules based on interfacial UV photodimerization. *Polym. Chem.* **2013,** 4, 1913-1920.
(49) Duan, H.; Wang, D.; Kurth, D. G.; Möhwald, H., Directing Self-Assembly of Nanoparticles at Water/Oil Interfaces. *Angew. Chem. Int. Ed.* **2004,** 43, 5639-5642.
(50) Tian, J.; Yuan, L.; Zhang, M.; Zheng, F.; Xiong, Q.; Zhao, H., Interface-Directed Self-Assembly of Gold Nanoparticles and Fabrication of Hybrid Hollow Capsules by Interfacial Cross-Linking Polymerization. *Langmuir* **2012,** 28, 9365-9371.
(51) Glaser, N.; Adams, D. J.; Böker, A.; Krausch, G., Janus Particles at Liquid−Liquid Interfaces. *Langmuir* **2006,** 22, 5227-5229.
(52) Binks, B. P.; Fletcher, P. D. I., Particles Adsorbed at the Oil−Water Interface: A Theoretical Comparison between Spheres of Uniform Wettability and "Janus" Particles. *Langmuir* **2001,** 17, 4708-4710.
(53) Fernandez-Rodriguez, M. A.; Ramos, J.; Isa, L.; Rodriguez-Valverde, M. A.; Cabrerizo-Vilchez, M. A.; Hidalgo-Alvarez, R., Interfacial Activity and Contact Angle of Homogeneous, Functionalized, and Janus Nanoparticles at the Water/Decane Interface. *Langmuir* **2015,** 31, 8818-8823.
(54) Aveyard, R., Can Janus particles give thermodynamically stable Pickering emulsions? *Soft Matter* **2012,** 8, 5233-5240.
(55) Fernández-Rodríguez, M. A.; Percebom, A. M.; Giner-Casares, J. J.; Rodríguez-Valverde, M. A.; Cabrerizo-Vílchez, M. A.; Liz-Marzán, L. M.; Hidalgo-Álvarez, R., Interfacial Activity of Gold Nanoparticles Coated with a Polymeric Patchy Shell and the Role of Spreading Agents. *ACS Omega* **2016,** 1, 311-317.

(56) Sashuk, V.; Hołyst, R.; Wojciechowski, T.; Fiałkowski, M., Close-packed monolayers of charged Janus-type nanoparticles at the air–water interface. *J. Colloid Interface Sci.* **2012,** 375, 180-186.
(57) Sashuk, V.; Winkler, K.; Żywociński, A.; Wojciechowski, T.; Górecka, E.; Fiałkowski, M., Nanoparticles in a Capillary Trap: Dynamic Self-Assembly at Fluid Interfaces. *ACS Nano* **2013,** 7, 8833-8839.
(58) Andala, D. M.; Shin, S. H. R.; Lee, H.-Y.; Bishop, K. J. M., Templated Synthesis of Amphiphilic Nanoparticles at the Liquid–Liquid Interface. *ACS Nano* **2012,** 6, 1044-1050.
(59) Lee, H.-Y.; Shin, S. H. R.; Abezgauz, L. L.; Lewis, S. A.; Chirsan, A. M.; Danino, D. D.; Bishop, K. J. M., Integration of Gold Nanoparticles into Bilayer Structures via Adaptive Surface Chemistry. *J. Am. Chem. Soc.* **2013,** 135, 5950-5953.
(60) Turek, V. A.; Cecchini, M. P.; Paget, J.; Kucernak, A. R.; Kornyshev, A. A.; Edel, J. B., Plasmonic Ruler at the Liquid–Liquid Interface. *ACS Nano* **2012,** 6, 7789-7799.

TOC Graphic